

## CFD Modeling to Improve the Design of a Fog System for Cooling Greenhouses

Keesung KIM<sup>1</sup>, Gene A. GIACOMELLI<sup>1</sup>, Jeong-Yeol YOON<sup>1</sup>,  
Sadanori SASE<sup>2\*</sup>, Jung-Eek SON<sup>3</sup>, Sang-Woon NAM<sup>4</sup> and In-Bok LEE<sup>5</sup>

<sup>1</sup> Department of Agricultural & Biosystem Engineering, University of Arizona  
(Tucson, AZ 85705, USA)

<sup>2</sup> Department of Rural Technologies, National Institute for Rural Engineering  
(Tsukuba, Ibaraki 305–8609, Japan)

<sup>3</sup> School of Plant Science, Seoul National University (Seoul 151–742, Korea)

<sup>4</sup> Department of Bioresources Engineering, Chungnam National University (Daejeon 305–764, Korea)

<sup>5</sup> Department of Rural System Engineering, Seoul National University (Seoul 151–742, Korea)

### Abstract

A CFD model was developed to simulate the air temperature and relative humidity distribution in greenhouses adopting fog-cooling systems using FLUENT. The developed model was validated using the data from a fog-cooling experiment in a single-span greenhouse without plants. The measured and simulated air temperatures varied from 0.1 to 1.4°C and the differences of relative humidity varied 0.3–6.0%. The validated model was then used to evaluate the design of a fog-cooling system in a multi-span glasshouse. The optimal system design was determined in terms of the cooling efficiency and the special uniformity of air temperature and relative humidity. The simulations demonstrated that the best performance of the cooling system occurred when the fog nozzles were located at the height of 2.3 m above the floor and at a distance of 1.9 m from the sidewalls with uniform row-to-row spacing of 3.7 m. The most effective location of the nozzles was within the air entry from the sidewall ventilator inlets of the greenhouse. However, it was important not to wet the sidewalls with the fog. This study suggested that the CFD model developed could be a useful tool to design and evaluate the fog-cooling systems in greenhouses with various configurations.

**Discipline:** Agricultural facilities

**Additional key words:** CFD, fog-cooling system, glasshouse, natural ventilation, wind speed

### Introduction

Evaporative cooling systems have been developed to provide the desired conditions for plant growth in the greenhouses during hot seasons. The fog system performs better than the pad-and-fan system with respect to uniform distribution of temperature and relative humidity in the greenhouse. The appropriate combination of air and water supply depends on the environmental conditions, such as solar radiation, ambient temperature and relative humidity, and is essential for maintaining the desired conditions in the greenhouse<sup>3</sup>.

The fog-cooling system supplies water droplets in diameters of 2–60 µm so as to enhance the heat and mass

exchange between the water and the air<sup>5</sup>. Ventilation is an important factor since the water spray evaporates along with the movement by airflow. Most studies on fog-cooling systems used forced ventilation systems<sup>3,4</sup>.

Natural ventilation is normally achieved by air exchanges through multiple controlled openings. Wind is generally the primary driving force in natural ventilation systems. System design and subsequent field-testing are very difficult due to the variations of environmental factors, wind velocity and direction, solar radiation, outside temperature, etc.<sup>7,13</sup>.

The Computational Fluid Dynamics (CFD) numerical technique has been widely used to study the airflow, air quality, and thermal conditions in greenhouses. These CFD simulations have several advantages compared to

---

This research was carried out under the US-Japan collaborative project on analysis and control of greenhouse environment for efficient crop production under semiarid climate.

\*Corresponding author: e-mail [sase@affrc.go.jp](mailto:sase@affrc.go.jp)

Received 8 September 2006; accepted 5 February 2007.

field experiments or indirect methods. Through the significant improvement in the 1990's, commercial CFD programs are capable of dealing with complicated turbulent flows. Short<sup>17</sup> first used the commercial CFD models to solve natural ventilation problems in a double-poly greenhouse. Mistriotis et al.<sup>14</sup> analyzed the ventilation process in greenhouses, without plants, using a CFD model. This study validated the CFD model by comparing the numerical airflow patterns with the experimental results of Sase et al.<sup>16</sup>.

Kacira et al.<sup>10</sup>, Al-Helal<sup>2</sup> and Lee & Short<sup>12</sup> studied various natural and mechanical ventilation systems using CFD models. These studies investigated the effects of various factors (weather conditions, greenhouse structure, internal and external shading screens, number of greenhouse spans, and the presence of plants as well as benches) on the air exchange rates in greenhouses. Lee & Short<sup>13</sup> verified the CFD simulations with the airflow and temperature distributions in a full-scaled naturally-ventilated multi-span greenhouse, suggesting that the CFD model can be a useful tool to evaluate the performance of the natural ventilation system.

The objectives of this study were to develop a two-dimensional CFD model to simulate temperature and relative humidity distributions, and to evaluate the performance of a fog-cooling system in a multi-span greenhouse. The CFD model was verified with the data from a naturally-ventilated fog-cooled single-span greenhouse and then was applied to a multi-span greenhouse for improving its cooling capabilities. The applicability of the CFD model to aid in the design of a fog-cooling system was also tested by evaluating various system conditions to determine an optimal system design based on the absolute cooling effect and the uniform distribution of air temperature and relative humidity.

## Materials and methods

### 1. Greenhouse configuration, fog system and measurements

A single-span and single-glass covered greenhouse without plants was designed for testing roof and sidewall ventilators in a natural ventilation system. The glasshouse was located at the city of Ansung in the middle of the Korean peninsula (Latitude: 37° 40", Longitude: 127° 28"). The greenhouse was 18 m in length, the span was 6.5 m, the height to the gutter was 2.4 m, and the roof angle was 22°. During the data collection periods, all ventilators were completely opened (Fig. 1). The air temperature and relative humidity were measured at three locations for each height of top (3.1 m), middle (2.25 m) and bottom (0.85 m) above the floor in the glasshouse

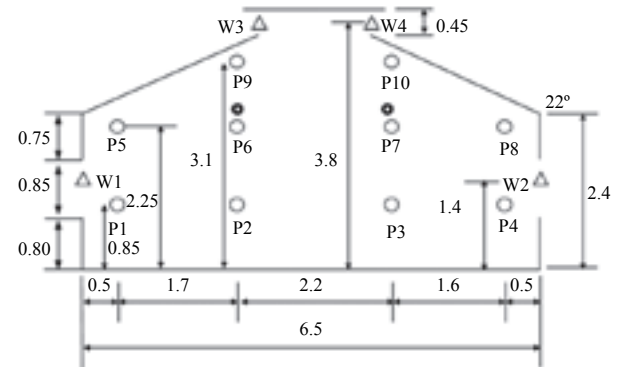


**Fig. 1. The schematics of the fog-cooling system in the greenhouse (unit: m)**

○ : Temperature and relative humidity,  
△ : Wind speed, ● : Fog nozzle.

every 10 s using HOBO sensors (Onset Computer Corp., USA). T-type thermocouples (OMEGA Engineering, Inc., USA) were used to measure the temperatures of glass walls, shade screens and floor. The airflow speeds were measured from side and roof windows in the longitudinal direction along the center of the greenhouse using an anemometer (Series 640, Dwyer Instrument, USA), while one-directional (x-velocity) speeds were measured for the airflow from the ventilation window (Fig. 1). The experiments were conducted in July through August in order to collect the data for the model validation. The environmental data during high radiation periods were used to verify the developed model.

The radiation sensors (LI200X, LI-COR, Inc., USA) were installed at the height of 3.2 m from the greenhouse floor to measure solar radiation. The temperatures by T-type thermocouples, airflow speeds and solar radiation values were stored to the data logger (HR2300, Yokogawa Electric Corp., Japan) as one-minute averages. A weather station (3.25 m height) was located 10 m away from the greenhouse to measure the external climate, including ambient air temperature (accuracy:  $\pm 0.05\%$ ) and relative humidity ( $\pm 2\%$  over 10–90%) (HMP45C, Campbell Scientific Inc., USA), wind speed ( $\pm 0.3 \text{ m}\cdot\text{s}^{-1}$ ) and wind direction (Model 05106, R.M. Young Company, USA), atmospheric pressure ( $\pm 0.05 \text{ kPa}$ , CS105, VAISALA, Finland), and solar radiation (waveband: 400–1,100  $\mu\text{m}$ ,  $\pm 5\%$ , LI200X, LI-COR, Inc., USA).

The design flow rate of the fog nozzle (Impaction pin IP-16, Mee Industries Inc., USA) was  $1.56 \text{ mL}\cdot\text{s}^{-1}$  at a pressure of 6,800 kPa, while the diameter of the spray measured at 90 cm from the nozzle was  $20 \mu\text{m}$ <sup>18</sup>. A total of 32 fog nozzles were installed with 1 meter spacing on two lines, one was located at 2.3 m from each sidewall and at a height of 2.4 m from the floor. The fog-cooling

system was operated for 45 s every 90 s from 10:00 to 16:00 without internal shading. The fog spray direction was vertically upward to increase the spray distance<sup>18</sup>.

**2. CFD numerical model**

The commercial CFD software (FLUENT<sup>®</sup>5.3 and GAMBIT<sup>®</sup>1.3, FLUENT Inc., Lebanon, New Hampshire, USA) was used to generate mathematical grids of the fog-cooling system in the greenhouse and numerically solve the Reynolds-averaged form of the Navier-Stokes equations<sup>8,11</sup> over each discrete flow field using the finite volume method (FVM). The Reynolds-averaged process considered the instantaneous fluid velocity to be the sum of a mean and a fluctuating component of turbulence<sup>6,9</sup>. Since the high frequency and small scale fluctuations of turbulence are very difficult to incorporate analytically, the modeling of turbulent flow related some or all of the turbulent velocity fluctuations to the mean flow quantities and their gradients. The standard  $\kappa$ - $\epsilon$  turbulence model was used for this study since this model has typically represented results from ventilation flows<sup>8,10,11</sup>. The turbulent viscosity,  $\mu_t$  is computed as a function of the turbulent kinetic energy ( $\kappa$ ) and the dissipation rate of turbulent kinetic energy ( $\epsilon$ ) in the standard  $\kappa$ - $\epsilon$  model.

In the vicinity of solid walls, the viscous effects are expected to be dominant over turbulent effects. Thus, this study applied wall functions by Launder & Spalding<sup>11</sup> in conjunction with the standard  $\kappa$ - $\epsilon$  equations. The walls were modeled as standard walls in the FLUENT program<sup>8,15</sup>.

The Discrete Ordinates (DO) model was chosen as a radiation model since it would consider the effects of light penetration through the transparent glass wall. The radiation was calculated once for every five computations of governing and turbulent equations<sup>18</sup>. The Boussinesq model was used to consider the issues regarding the gravitation and energy<sup>8</sup>.

The Discrete Phase model was designed to analyze the changes of the thermal environment by the spray particles in the fluid. This model allowed tracking of the moving path of spray particles and analysis of the heat transfer for the fog-cooling system in the greenhouse. Three options were available for selecting the types of spray particles, including inert, droplet and combusting types. We chose the droplet type to simulate the evaporation of fog<sup>8</sup>. Using the Discrete Phase model, the effect of a spray fog on the thermal environment was calculated every calculation of the governing equation until repeated 100 times. The Unsteady-tracking option was used to simulate the intermittent operation of the fog system by specifying the operation and non-operation periods applied to the experiments. The Multi-species model

option was used to mimic the moist air, a mixture of air and water particles. In addition, the option to consider the reaction of the sprayed fog to solar radiation was applied<sup>8</sup>. The parameters of air physical characteristics such as specific heat, heat transfer coefficient, viscosity, etc., were found from previous studies or the database supplied by the Fluent program and used for the simulation. The option, Mass fraction of H<sub>2</sub>O was used to present the distribution of relative humidity in the greenhouse<sup>8</sup>. Mass fraction of H<sub>2</sub>O is the ratio of the mass of H<sub>2</sub>O to the total mass of moist air (dry air + vapor). This fraction was converted first to humidity ratio, which then was converted to relative humidity<sup>1</sup>.

Table 1 presents the basic components of the CFD model. The physical parameters of the building materials are summarized in Table 2. The external climatic data for the wind directions which were perpendicular ( $\pm 10^\circ$  variations) to the sidewalls of the greenhouse were used for the simulation, while the high and steady solar radiation during the daytime was applied (Table 3).

The external wind speeds and directions were measured from the weather station and applied for the left-side boundary conditions in the form of “velocity-inlet”. Turbulent characteristics of fluid were specified by the intensity and length of turbulence. Turbulence intensities were applied by 5% and 1% for the wind speed greater and less than 2 m·s<sup>-1</sup>, respectively<sup>2</sup>, while the turbulence length of 3.5 m was used for the simulation<sup>13</sup>. The venti-

**Table 1. The basic components of the CFD model**

Classification	Setting of Method
Solver	Segregated solver 2D simulation Implicit formulation Absolute velocity formation Unsteady state analysis (1st-order implicit)
Energy equation	Activated
Viscous model	Standard $\kappa$ - $\epsilon$ model Standard wall functions Full buoyancy effects
Radiation model	DO (Discrete Ordinates) Theta divisions: 2 Phi divisions: 2 Heta pixels: 1 Phi pixels: 1 Non-gray model: non-selected Iteration ratio (flow/radiation): 5
Species model	Multiple species
Discrete phase model	Activated
Multiphase model	Activated
Pollutants	Inactivated

**Table 2. Physical properties of materials at the temperature of 300 K**

Physical property (unit)	Soil	Glass	Concrete
Density ( $\text{kg}\cdot\text{m}^{-3}$ )	1,900	2,700	2,100
Specific heat ( $\text{J}\cdot\text{kg}^{-1}\cdot\text{K}^{-1}$ )	2,200	840	880
Thermal conductivity ( $\text{W}\cdot\text{m}^{-2}\cdot\text{K}^{-1}$ )	2.0	0.78	1.4
Absorption coefficient	0.5	0.1	0.6
Scattering coefficient	1	0	1
Refractive index	1	1	1
Emissivity	0.89	0.90	0.71

**Table 3. Input parameters for the CFD model to simulate a fog-cooling system**

Input variable (unit)	Values
Temperature of air through inlet (K)	303.85
Relative humidity of air through inlet (%)	58.9
Outside radiation ( $\text{W}\cdot\text{m}^{-2}$ )	678
Speed of air through inlet ( $\text{m}\cdot\text{s}^{-1}$ )	0.44
Wind direction	Left to right
Saturated vapor pressure (Pa)	4,430
Wet bulb temperature of air through inlet (K)	298.35
Spraying water temperature (K)	297.45
Spraying time (s)	45
Spraying interval (s)	45
Spraying water amount ( $\text{kg}\cdot\text{s}^{-1}\cdot\text{nozzle}^{-1}$ )	0.00157
Evaporation percentage (%)	70.8
Droplet size ( $\mu\text{m}$ )	20

**Table 4. Comparison of measured and simulated environmental factors at each measurement point (1–9: Fig. 1)**

Factor point	Temperature			Relative humidity		
	Measured ( $^{\circ}\text{C}$ )	Simulated ( $^{\circ}\text{C}$ )	Error* ( $^{\circ}\text{C}$ )	Measured (%)	Simulated (%)	Error* (%)
1	32.0	30.8	+1.2 (3.8)	60.3	66.1	-5.8 (9.6)
2	30.8	29.4	+1.4 (4.4)	72.5	72.0	+0.5 (0.7)
3	30.1	30.2	-0.1 (0.5)	72.5	67.2	+5.3 (7.3)
4	32.8	32.2	+0.6 (1.7)	58.0	57.7	-0.3 (0.6)
5	30.9	29.9	+1.0 (3.3)	66.1	69.5	-3.4 (5.2)
6	30.8	31.3	-0.5 (1.5)	66.6	60.6	+6.0 (9.0)
7	31.1	31.8	-0.7 (2.2)	63.3	58.8	+4.5 (7.1)
8	29.2	30.1	-0.9 (3.0)	70.7	65.7	+5.0 (7.0)
9	33.8	32.7	+1.1 (3.3)	55.3	55.7	-0.4 (0.7)

\*: Standard error (%).

lator was specified by “interior” as an entry of external air into the greenhouse. The “pressure-outlet” option was applied for the right-side boundary conditions so that the pressure gradient becomes the driving force for the air movement. The measured solar radiation data were used for the upper boundary conditions using the option of “wall”.

## Results and discussions

### 1. Validation of CFD model

Measured and simulated air temperature and relative humidity at each measurement point are presented in Table 4. The standard errors of temperatures were 0.5 to 4.4%. The measured temperatures were greater than the simulations in the vicinity of the sidewalls and the roof in

the greenhouse. This is because the effects of heat transfer through the walls were dominant in these areas. Most evaporation of the sprayed fog also appeared to take place in lower parts of the greenhouse as the water droplet falls down. The standard errors of relative humidity between the measurements and the simulations varied from 0.6% to 9.6%. Overall greater relative humidity was observed from the lower portion as compared to the upper portion of the greenhouse due to the evaporation of dropped water particles. Figures 2 and 3 illustrate the temperature and humidity distributions, respectively, in the greenhouse by comparing the measured and simulated values. The contour lines were generated using the surfer software (Version 6, Golden Software, Inc., USA). The simulations by the CFD model showed similar values with the measurements.



Fig. 2. Comparison of measured (left) and simulated (right) temperature in the greenhouse



Fig. 3. Comparison of measured (left) and simulated (right) relative humidity in the greenhouse

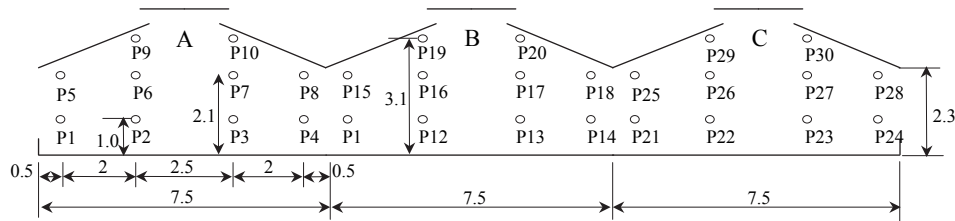


Fig. 4. Dimension of the greenhouse and specific calculation points for simulation (unit: m)

○ : Temperature and relative humidity calculation points.

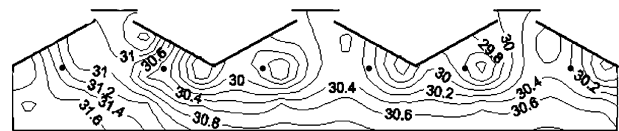
## 2. Simulation for a multi-span glasshouse

The verified CFD model was applied to evaluate the fog-cooling system in a three-span greenhouse with a span of 7.5 m, a height to the gutter of 2.3 m, and a roof angle of 28°. The different nozzle locations with several external wind speeds were simulated to find an optimal configuration of the fog-cooling system (Fig. 4). Gambit was used to generate the computational grids of the greenhouse. The temperature and relative humidity were simulated at a total of 30 points, 10 points for each span using the CFD model. The cooling efficiency of the greenhouse was also estimated for the different nozzle locations and external wind speeds.

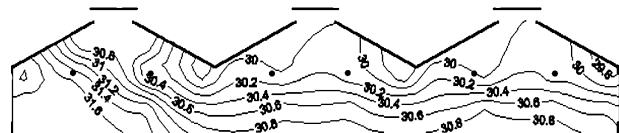
The simulations were repeated with different nozzle locations to evaluate the effects of nozzle locations on the cooling efficiency. The nozzle locations used for the simulations are presented in Fig. 5. The nozzles were located at specified certain intervals from the left-side wall of the greenhouse, which directed the fog spray into the incoming air stream. The nozzles were located at the highest point, but not to have them reach the roof. The fog was projected vertically upward in order to maximize the falling length of the droplets. The amount of spray water was determined based on the target temperature of 30°C which is generally used for summer in Korea. Table 5 summarizes the external climatic data used for the simulations.

- (1) Internal environment changes depending on the nozzle locations

The temperature distributions in the greenhouse corresponding to the nozzle locations were simulated (Fig. 5). Table 6 contains the mean values of air temperature and relative humidity for each span of the greenhouse, A,



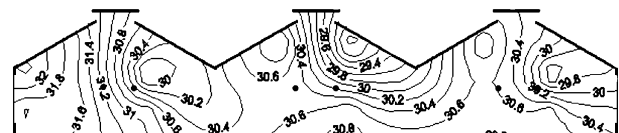
(a) Case 1: nozzle locations of 1.9, 5.6, 9.4, 13.1, 16.9, and 20.6 m from the left wall at the height of 2.3 m with the vertical-upward injection of spray.



(b) Case 2: nozzle locations of 2.35, 5.15, 9.85, 12.65, 17.35, and 20.15 m from the left wall at the height of 2.5 m with the vertical-upward injection of spray.



(c) Case 3: nozzle locations of 2.8, 4.7, 10.3, 12.2, 17.8, and 19.7 m from the left wall at the height of 2.7 m with the vertical-upward injection of spray.



(d) Case 4: nozzle locations of 3.25, 4.25, 10.75, 11.75, 18.25, and 19.25 m from the left wall at the height of 3.0 m with the vertical-upward injection of spray.

Fig. 5. The temperature distributions corresponding to the nozzle locations

● : Nozzle location.

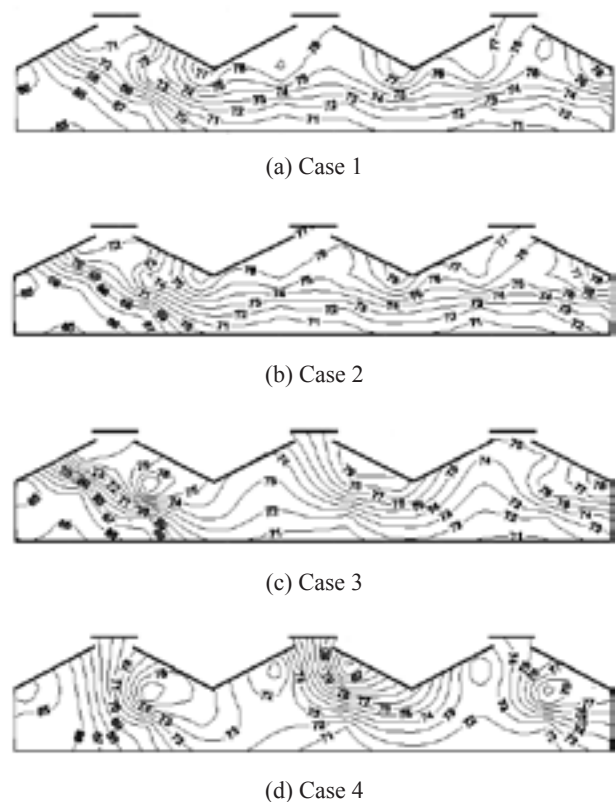
B and C. The average temperatures in the greenhouse approached the target temperature of 30°C and were similar for all the conditions. However, the average temperature of span A was greater than those of spans B and C. The movement of the sprayed droplets from span A to spans B and C along with the air current was considered as the primary cause of the temperature difference. As shown in Fig. 5, Case 1 showed the most uniform temperature distribution as compared to the other cases. Consequently, the nozzle should be located the closest to the sidewall, unless the spray reaches the sidewall, in order to consider the spray movement along with the air inflow. The plant canopy should be considered to determine the height of the nozzle locations. The vertical-upward injection appeared to improve the evaporation of the sprayed droplets by maximizing the dropping distance.

Figure 6 illustrates the distributions of relative humidity in the greenhouse corresponding to the nozzle

locations. The average means of relative humidity in span A were approximately 5% lower than those in spans B and C, regardless of the nozzle locations. The movement of the sprayed droplets from span A to B and C by the air-flow again appeared to be the primary reason. Case 1 showed the most uniform distribution of relative humidity as compared to the other cases. According to Arbel et al.<sup>3</sup>, the uniform spacing of the nozzles at the height of the gutter demonstrated the uniform distributions of temperature and relative humidity in the greenhouse.

**Table 5. Input data for the CFD model to simulate the fog-cooling system in the multi-span greenhouse**

Input variable (unit)	Value
Temperature of air through inlet (K)	305.75
Relative humidity of air through inlet (%)	60.1
Outside radiation ( $W \cdot m^{-2}$ )	881
Speed of air through inlet ( $m \cdot s^{-1}$ )	0.35
Wind direction	Left to right
Saturated vapor pressure (Pa)	4,490
Wet bulb temperature of air through inlet (K)	299.25
Spraying water temperature (K)	291.15
Spraying time (s)	55
Spraying interval (s)	75
Spraying water amount ( $kg \cdot s^{-1} \cdot nozzle^{-1}$ )	0.00157
Evaporation percentage (%)	80
Droplet size ( $\mu m$ )	20



**Fig. 6. The distributions of relative humidity in the greenhouse for each condition**

**Table 6. The mean values of temperature and relative humidity in the spans A, B and C depending on the nozzle locations**

Span	Case 1		Case 2		Case 3		Case 4	
	Temperature (°C)	Relative humidity (%)	Temperature (°C)	Relative humidity (%)	Temperature (°C)	Relative humidity (%)	Temperature (°C)	Relative humidity (%)
A	31.0	69.8	31.0	69.8	30.9	70.6	31.0	69.8
B	30.2	74.8	30.2	74.8	30.2	74.6	30.2	74.7
C	30.2	75.0	30.2	75.0	30.3	74.4	30.3	74.6
Max	31.3	77.1	31.3	77.0	31.3	76.5	31.1	77.5
Min	29.7	67.8	29.9	67.8	30.0	68.0	30.0	69.0
Mean	30.4	73.2	30.5	73.2	30.5	73.2	30.5	73.0

(2) Internal environmental changes in response to the external wind speed changes

Actual meteorological conditions, especially the wind speed, are changing continuously. Therefore, the series of simulations with different external wind speeds were conducted to investigate the effects of the external wind speed on the cooling efficiency. The air entry speeds, 0.1, 0.5, 1.0, and 2.0 m·s<sup>-1</sup> were used for the simulations with the fixed nozzle locations as in Case 1 of Fig. 5. Table 7 presents the mean values of temperature and relative humidity in the greenhouse with respect to the wind

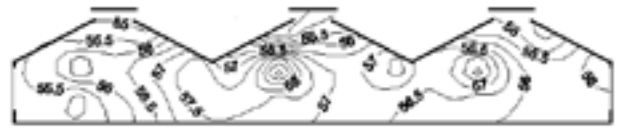
speed changes. Except for wind speed of 0.1 m·s<sup>-1</sup> the mean temperatures were close to the target temperature of 30°C. The wind speed of 0.1 m·s<sup>-1</sup> (Case 5), showed approximately 4°C greater average temperature than the target temperature. The low wind speed appeared to cause the insufficient ventilation in the greenhouse. Subsequently, the decreased air movement seemed to reduce the evaporation by decreasing the moving distance of the droplets. As the wind speed increased up to 1 m·s<sup>-1</sup>, the mean temperatures in the greenhouse were decreased. Figures 7 and 8 depict the distributions of temperature and

**Table 7. The mean values of temperature and relative humidity in different wind speeds**

Wind speed (m·s <sup>-1</sup> )	Case 5 0.1		Case 6 0.5		Case 7 1.0		Case 8 2.0	
	Temperature (°C)	Relative humidity (%)	Temperature (°C)	Relative humidity (%)	Temperature (°C)	Relative humidity (%)	Temperature (°C)	Relative humidity (%)
A	34.4	56.3	31.0	70.0	30.0	74.8	30.2	73.0
B	34.4	57.0	30.2	74.9	29.1	81.0	29.2	80.2
C	34.7	56.1	30.1	76.1	28.8	83.1	28.9	81.8
Mean	34.5	56.5	30.4	73.7	29.3	79.6	29.4	78.3



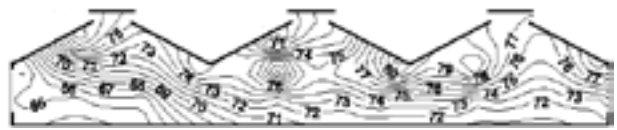
(a) Case 5 (wind speed: 0.1 m·s<sup>-1</sup>)



(a) Case 5 (wind speed: 0.1 m·s<sup>-1</sup>)



(b) Case 6 (wind speed: 0.5 m·s<sup>-1</sup>)



(b) Case 6 (wind speed: 0.5 m·s<sup>-1</sup>)



(c) Case 7 (wind speed: 1.0 m·s<sup>-1</sup>)



(c) Case 7 (wind speed: 1.0 m·s<sup>-1</sup>)



(d) Case 8 (wind speed: 2.0 m·s<sup>-1</sup>)



(d) Case 8 (wind speed: 2.0 m·s<sup>-1</sup>)

**Fig. 7. The distributions of temperature corresponding to the external wind speed**

**Fig. 8. The distributions of relative humidity corresponding to the external wind speed**

relative humidity, respectively. Case 6 of which the wind speed was  $0.5 \text{ m}\cdot\text{s}^{-1}$  showed the most uniformity in temperature. With wind speed greater than  $0.5 \text{ m}\cdot\text{s}^{-1}$ , the air temperature decreased below the desired level and the vertical temperature differences occurred by approximately  $2^\circ\text{C}$ . Although Case 5 showed the most uniform distribution of relative humidity, the overall mean values of relative humidity was 56.5%, which was relatively low. This might be the result of the decreased evaporation of the water droplets as described earlier. However, as the wind speed increased above  $0.5 \text{ m}\cdot\text{s}^{-1}$ , the gradients of relative humidity from span A to C, from the lowest to the highest, occurred due to the droplets' movement along with airflow (Table 7). The most desirable distribution of relative humidity was derived from the wind speed of  $0.5 \text{ m}\cdot\text{s}^{-1}$  (Case 6). Arbel et al.<sup>4</sup> reported that the entry velocity of the air into the greenhouse should not exceed about  $0.5 \text{ m}\cdot\text{s}^{-1}$  in order to obtain uniform environmental conditions in the greenhouse.

## Conclusions

In this study, a CFD model was developed to model a fog-cooling system in a greenhouse using Fluent<sup>®</sup>5.3. The data obtained from an experiment of a fog-cooling system in a single-span greenhouse were used to verify the CFD model. The model and actual measurements showed differences of  $0.1$  to  $1.4^\circ\text{C}$  in temperature and  $0.3$  to  $6.0\%$  in relative humidity. The verified model was used to evaluate the cooling efficiency and to find an optimal setup of the fog-cooling system to give the most uniform temperature and relative humidity in a multi-span glasshouse. The best performance of the fog-cooling system was when the fog nozzles were located at the height of  $2.3$  m from the floor and  $1.9$  m from the sidewalls with the spacing of  $3.7$  m. The closest nozzle location to the sidewall, without the sprayed droplets reaching the sidewall, appeared to give the best performance of the fog-cooling system. The air entry speed of  $0.5 \text{ m}\cdot\text{s}^{-1}$  resulted in the highest uniformity in temperature and relative humidity in the greenhouse. The developed CFD model can be a useful tool to evaluate and design fog-cooling systems in greenhouses with various configurations.

## References

1. Albright, L. D. (1990) Environment control for animals and plants. ASAE, St. Joseph, USA, pp.453.
2. Al-Helal, I. M. (1998) A computational fluid dynamics study of natural ventilation in arid region greenhouses. Ph.D. diss. Ohio State University, Columbus, USA, pp.186.
3. Arbel, A., Yekutieli, O. & Barak, M. (1999) Performance of a fog system for cooling greenhouses. *J. Agric. Eng. Res.*, **72**, 129–136.
4. Arbel, A., Barak, M. & Shklyar, A. (2003) Combination of forced ventilation and fogging systems for cooling greenhouses. *Biosystems Eng.*, **84**(1), 45–55.
5. ASHRAE (1972) Environmental control for animals and plants. In ASHRAE handbook of fundamentals, ASHRAE, Atlanta, USA, 177–186.
6. Bennet, C. O. & Myers, J. E. (1995) Momentum, heat and mass transfer. McGraw-Hill, New York, USA, pp.848.
7. Campen, J. B. & Bot, G. P. A. (2003) Determination of greenhouse-specific aspects of ventilation using three-dimensional computational fluid dynamics. *Biosystems Eng.*, **84**(1), 69–77.
8. Fluent Inc. (1998) FLUENT 5 user's guide. Lebanon, USA. Available online at <http://venus.imp.mx/hilario/SuperComputo/Fluent.Inc/manuals/fluent5/ug/>.
9. Hinze, J. O. (1975) Turbulence, 2nd ed. McGraw-Hill, New York, USA, pp.790.
10. Kacira, M., Short, T. H. & Stowell, R. R. (1998) A CFD evaluation of naturally ventilated, multi-span, sawtooth greenhouses. *Trans. ASAE*, **41**(3), 833–836.
11. Launder, B. E. & Spalding, D. B. (1974) The numerical computation of turbulent flows. *Comp. Methods Appl. Mech. Eng.*, **3**, 269–289.
12. Lee, I. & Short, T. H. (2000) Two-dimensional numerical simulation of natural ventilation in a multi-span greenhouse. *Trans. ASAE*, **43**(3), 745–753.
13. Lee, I. & Short T. H. (2001) Verification of computational fluid dynamic temperature simulations in a full-scale naturally ventilated greenhouse. *Trans. ASAE*, **44**(1), 119–127.
14. Mistriotis, A. et al. (1997) Analysis of the efficiency of greenhouse ventilation using computational fluid dynamics. *Agric. For. Meteorol.*, **85**, 217–228.
15. Patankar, S. V. (1981) A calculation procedure for two-dimensional elliptic situations. *Numer. Heat Transfer*, **4**(4), 409–425.
16. Sase, S., Takakura, T. & Nara, M. (1984) Wind tunnel testing on airflow and temperature distribution of a naturally ventilated greenhouse. *Acta Hortic.*, **148**, 329–336.
17. Short, T. H. (1996) Selecting the greenhouse structure your crop needs. *GrowerTalks*, Summer Issue, July, 8–9.
18. Yu, I. H. (2002) Development of CFD model for estimation of cooling effect of fog cooling system in greenhouse. *J. Bio-environ. Control*, **11**(2), 93–100.